

Nonlinear Response-History Analysis of Triple Friction Pendulum Bearings (TFPB), Installed Between Stories

Hamidreza. Fakhri

MSc of Earthquake Engineering , Building and Housing Research Center, Tehran, Iran

Gholamreza. Ghodrati Amiri

Professor, School of Civil Engineering, Iran University of Science & Technology - Aryan Institute of Science & Technology, Iran



SUMMARY:

In recent years, the damage to the well-designed structures, caused by earthquake, has attracted the attention of engineers to use adaptive seismic isolation systems such as Triple Friction Pendulum Bearings (TFPBs). An adaptive seismic isolator can exhibit different stiffness and damping during its course of motion and consequently award appropriate performance in different hazard levels. This paper investigates application of TFPBs in six stories steel frame structure, while TFPBs is installed at different levels; such as base, first story, third story or combination of them, and each state is compared with fixed-base and base isolated structure. The results indicate that base and first story isolation systems are extremely effective in reduction of maximum drift ratio and story shear force however this effect is diminished by increasing level of isolators. Additionally providing a second isolation level to base isolated structure, leads to a significant reduction in base deformation which is an adequate technique in presence of near-fault ground motion.

Keywords: Triple Friction Pendulum Bearing (TFPB), inter-story isolation system, multi-story isolation system

1-INTRODUCTION

Triple Friction Pendulum Bearing (TFPB) is the most matured friction pendulum bearings, which can exhibits different stiffness and damping during its course of motion. TFPB presents improved hysteretic characteristic to control performance over broad range of excitation (Fenz & Constantinou, 2008). Single Friction Pendulum Bearing (SFPB) as a first generation of friction pendulum bearings were invented by Zayas in 1986 and since that time many researches have been conducted to improve seismic performance of SFPB. In this regard, Double Friction Pendulum Bearing (DFPB) and finally Triple Friction Bearing are developed and many researches supported their adaptive behavior during earthquake (Constantinou & Fenz, 2008). Comprehensive researches have been performed by Fenz & Constantinou about force-displacement behaviors and sliding regimes for different types of friction isolators, especially for TFPB bearings. They have simulated behavior of TFPB system with three equivalent single-friction pendulum elements which connected in series and its advantages have been proved by experimental tests (Figure 1).

Most of seismic isolation systems in new buildings have been installed in base level, however for retrofitting purpose inserting device in this level could be more complicated and expensive. Installing isolators in higher levels as a strategy have advantages such as; the possibility of changing column arrangements and serviceability for upper stories of isolation level. Further, lower cost and disturbance for residents during retrofit are other advantages of using isolation system between stories.

Shirayama et al. (2004) investigated seismic behaviors of inter-story isolation systems through numerical studies. They concluded that effects of the inter-story isolation systems can be significantly related to the plastic behaviors of inter-story isolators. Ryan and Earl in 2010 systematically examined the effectiveness and feasibility of inter-story isolation systems as a function of their location, and proposed alternative approaches for selecting their properties. They showed Single-story isolation systems using Lead Rubber Bearings (LRB) at any levels are quite effective in mitigating force demands above the isolation system but less effective in mitigating lower-level forces (Ryan & Earl, 2010). In 2012, Charmpis et al. tried to formulate the research for favorable configurations of friction isolators at various story levels. They had a numerical study using time-history analyses of a typical six-story building. They accomplished this research with the optimization approach remarked that base isolation alone always yields higher absolute floor accelerations than the optimized isolation configurations. They showed for very strong earthquakes, base isolation demands a huge seismic gap, which is usually impractical (Charmpis & Komodromos, 2012).

Herein, behavior of TFPB is modeled in sap2000 (reference) and seismic response of six-story steel frame is investigated when TFPBs are located at different levels.

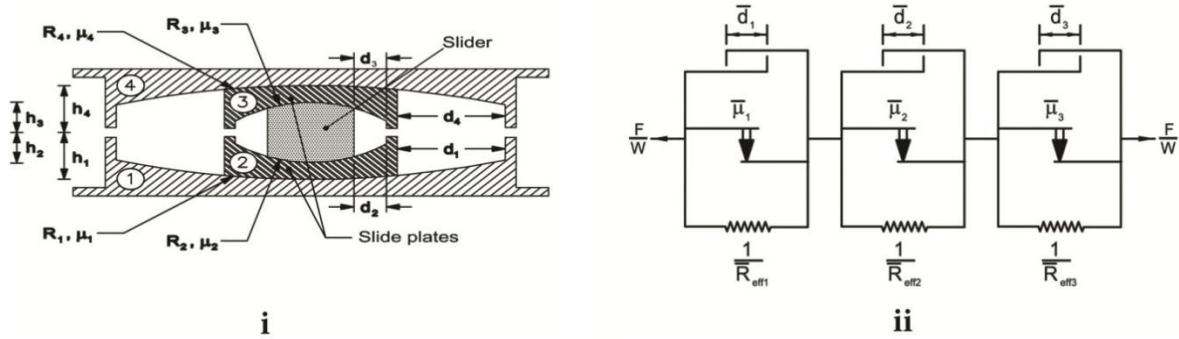


Figure 1. (i) Cross section of the triple FP bearing labeled with parameters that dictate behavior. R_i is the radius of curvature of surface i , h_i is the radial distance between the pivot point and Surface i and μ_i is the coefficient of friction at the sliding interface. (ii) three single FP elements in series used to model the behavior of the triple FP bearing.

2. ADAPTIVE BEHAVIOR OF TRIPLE FRICTION PENDULUM BEARING

A cross section of triple friction isolator and schematic of three single FP elements connected in series have been shown in fig. 1. Applied force on each element (single FP isolators) is the same but displacements are different. Each single FP element consists of a parallel arrangement of (a) a linear elastic spring element representing the restoring force provided by the curvature of the spherical dish, (b) a rigid plastic friction element with velocity dependence, and (c) a gap element to account for the finite displacement capacity of each sliding surface. For element i of fig. 1(ii), the stiffness of the spring is given by $\frac{1}{\bar{R}_{eff i}}$ where $\bar{R}_{eff i}$ is the effective radius of curvature, the velocity dependent coefficient of friction is $\bar{\mu}_i$ and the displacement at which the gap element engages is \bar{d}_i . Here, overbar notation is used to denote parameters and responses associated with the series model and standard notation is used to denote parameters and responses associated with the true behavior of the triple FP bearing. (Fenz & Constantinou, 2008)

Displacement of series i element (in figure 1(ii)) will initiate, when horizontal force F exceeds the friction force, $F_{fr} = \bar{\mu}_i W$ where W is the vertical load supported by bearing, and element movement will be stopped when displacement became equal with displacement capacity of each gap elements.

Consequently, loads at the beginning of movement and end of movement for each element will be extracted respectively from $\bar{F}_{fi} = \bar{\mu}_i \cdot w$ and $\bar{F}_{dri} = \frac{w}{R_{effi}} \bar{d}_i + \bar{F}_{fi}$. Details of equations for five sliding regimes have illustrated in MCEER report (Constantinou & Fenz, 2008). If parameters of each element are selected under the condition of $\bar{F}_{f1} < \bar{F}_{f2} < \bar{F}_{f3} < \bar{F}_{dr2} < \bar{F}_{dr3}$ then, displacement-force behavior of series isolators will be as triple friction pendulum bearing behavior. All Five sliding regimes of a triple friction pendulum isolator are shown in fig. 2. Isolator system response will be optimum and all five sliding regimes will work properly, if seismic magnitude be enough big and the value of gap elements are chosen carefully.

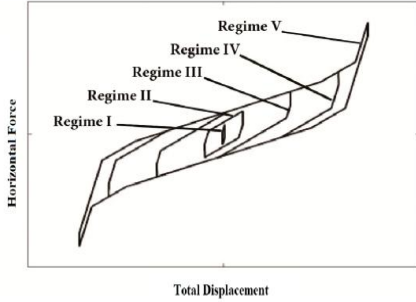


Figure 2. Five full sliding regime of a triple isolator

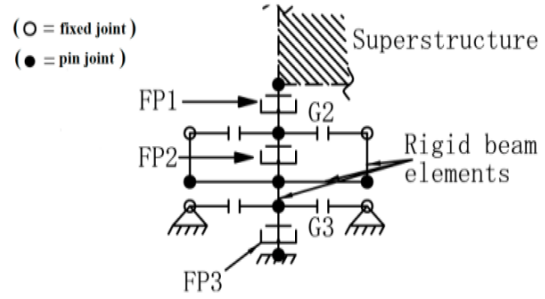


Figure 3. Assembly of friction pendulum link elements, gap elements and rigid beam elements used to model the behavior of the triple FP bearing in software used

For calculating of series model parameters, it has been assumed that, triple FP bearing works full adaptive, its means that all five sliding regimes shown in fig. 2 are included. Triple FP bearing will work fully adaptive, if following four conditions can be admitted:

$$R_{eff2} = R_{eff3} \ll R_{eff1} = R_{eff4} \quad (1)$$

$$\mu_2 = \mu_3 < \mu_1 < \mu_4 \quad (2)$$

$$d_2 > (\mu_1 - \mu_2)R_{eff2} \quad (3)$$

$$d_3 > (\mu_4 - \mu_3)R_{eff3} \quad (4)$$

In proposed series model (see fig. 1(ii)), first FP element represents the combined behavior of inner surfaces 2 and 3, ($\bar{\mu}_1 = \mu_2 = \mu_3$) while the second and third elements represent the external surfaces of 1 and 4 respectively ($\bar{\mu}_2 = \mu_1, \bar{\mu}_3 = \mu_4$).

3. MODELING AND VERIFICATION OF MODEL

Triple friction pendulum bearing can't be modeled directly in sap2000 software, but single friction pendulum bearing could be modeled by this software. As mentioned in the proposed model of Fenz and Constantinou (Fenz & Constantinou, 2008), triple FP bearing could be simulated based on three single FP bearings. Arrangement of gap elements and rigid beam elements with two-joint FP link is proposed for triple FP bearing modeling. This arrangement has been shown in fig. 3. Displacement capacity for gap elements G2 and G3 are \bar{d}_2 and \bar{d}_3 respectively. Arrangement of rigid beam elements is required for G2 element to be able to engage with relative displacement \bar{d}_2 . The gap elements are pin-ended to approximately model the capability of the slider to rotate freely when against the displacement restrainer. The overall height of the entire assembly is equal to the height of the actual bearing (Fenz & Constantinou, 2008).

Characteristics of triple FP bearing used for modeling verification have been sorted in Table 1.

Table 1. Characteristics of bearing used for modeling verification (Fenz & Constantinou, 2008).

Actual properties from testing (Constantinou & Fenz, 2008)				
Surface 1	$R_{eef1} = 435 \text{ mm}$	$\mu_1=0.02-0.04$	$d_1=64 \text{ mm}$	$a_1=0.1 \text{ sec/mm}$
Surface 2	$R_{eef2} = 53 \text{ mm}$	$\mu_2=0.01-0.02$	$d_2=19 \text{ mm}$	$a_2=0.1 \text{ sec/mm}$
Surface 3	$R_{eef3} = 53 \text{ mm}$	$\mu_3=0.01-0.02$	$d_3=19 \text{ mm}$	$a_3=0.1 \text{ sec/mm}$
Surface 4	$R_{eef4} = 435 \text{ mm}$	$\mu_4=0.06-0.13$	$d_4=64 \text{ mm}$	$a_4=0.1 \text{ sec/mm}$
Properties of series elements				
Element 1	$\bar{R}_{eff1}=106 \text{ mm}$	$\bar{\mu}_1=0.01-0.02$	$\bar{d}_1= -$	$\bar{a}_1=0.05 \text{ sec/mm}$
Element 2	$\bar{R}_{eff2}=382 \text{ mm}$	$\bar{\mu}_2=0.02-0.04$	$\bar{d}_2=56.2 \text{ mm}$	$\bar{a}_2=0.11 \text{ sec/mm}$
Element 3	$\bar{R}_{eff3}=382 \text{ mm}$	$\bar{\mu}_3=0.06-0.13$	$\bar{d}_3=56.2 \text{ mm}$	$\bar{a}_3=0.11 \text{ sec/mm}$

Parameters like coefficient of friction, radius of curvature and gap element size are important properties because they control overall behavior and isolator response, conclusions of prepared modeled have been compared with results of a three-dimensional single-span frame which has been analyzed by Fenz & Constantinou for model verification. Frame specification and applied load are as follow:

A one story building with superstructure weight 133.3kn, period 0.2sec and damping %0.25. Unidirectional excitation along one axis of the building is applied using the 180 component of the 1940 El Centro record (PGA of 0.31 g) available from the PEER NGA database. The motion was scaled by a factor of 2.15, which was chosen only to induce isolator displacements that were large enough to show all possible sliding regimes (Fenz & Constantinou, 2008). Other specifications have been shown in fig. 4.

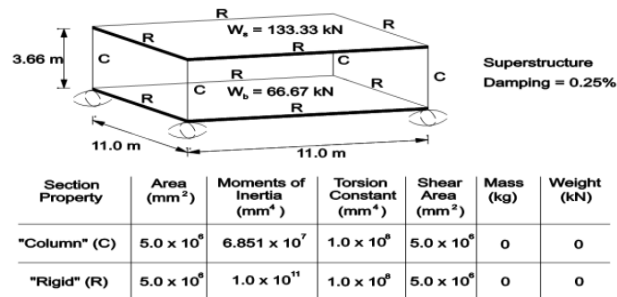


Figure 4. Description of simple seismically isolated structure for model verification (Fenz & Constantinou, 2008).

Hysteresis curve for this research and research done by Fenz & Constantinou have been illustrated in fig. 5. It can be conclude that two curves are compatible.

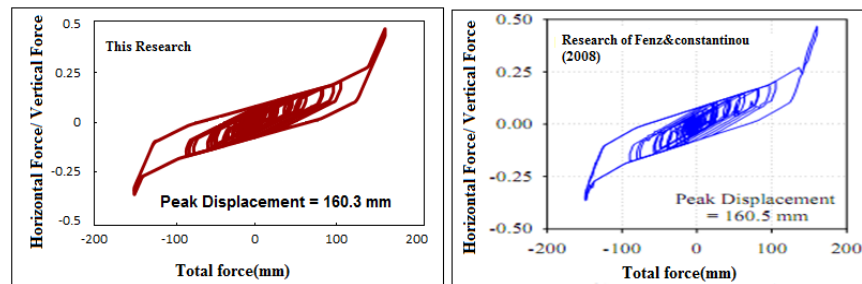


Figure 5. Comparison of hysteresis curves, this paper (lift), research by Fenz & Constantinou (right) (Fenz & Constantinou, 2008).

4. MODEL CHARACTERISTICS

Investigated frame in this research is a steel six-story shear frame (infinity rigid beams) which has been used for similar research on LRB isolators, (Ryan & Earl, 2010) this frame illustrate in fig. 6(i). Equal constant mass m assigned to each level. The story stiffness, k_i , are distributed such that $k_1 = k_2 = k$, $k_3 = k_4 = \frac{7}{8} * k$ and $k_5 = k_6 = \frac{3}{4} * k$, and k is scaled to give the reference structure (frame g) a fundamental period $T_n = 0.5$ sec. mass is assigned as shown in fig. 6(ii), where the total mass at an isolation level may exceed the mass m at a typical level due to extra measures taken to stiffen the structure just below the isolation system. This additional mass m_a (fig. 6(ii)) is set to $0.1m$. (Ryan & Earl, 2010)

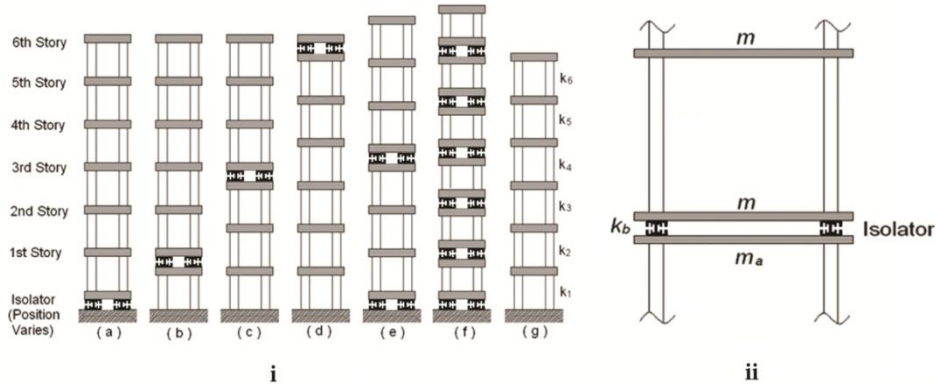


Figure 6. (i) Investigated six-story steel frame (ii) mass distribution for suggested inter-story isolation system.

The frame span is 25ft (7.62m), story height is 15ft (4.57m), dead load on each story is 60 lb/ft² Live load participation factor is 25% and total load on each isolator at the base level is about 375kn. Damping 2% has been assigned for structure in isolation level for first and fourth mode. General specification and loading conditions have been considered for minimum uplift and for more accuracy; damping 99% has been assigned for modes which have uplift. Selected frame has been design when isolators installed at base. For time history analyze, records of far field with soil type D are selected from ATC-63. Specification of records and scale factors are shown in Table 2. Figure 7 presents a comparison of the average 5% damped spectra of the scaled ground motions and the target design spectrum. For scaling to MCE level, scaling factors have been multiplied by 1.5.

The rate parameter, a , and friction coefficient, μ , for isolators in this paper, are like those in Constantinou's paper (see Table1), but gap elements and effective radius of curvature are listed in Table 3. Specification of isolators will not disturb the adaptive behavior of isolation system.

Table 2. Specification of records.

Earthquake		Recording Station		PGA(g)	Scale factor(DBE)
Name	Year	Name	Owner		
Northridge	1994	Beverly Hills	USC	0.52	0.962
Imperial Valley	1979	El Centro Array #11	USGS	0.38	1.316
Kobe	1995	Shin-Osaka	CUE	0.24	2.083
Landers	1992	Cool water	SCE	0.42	1.191
Loma Prieta	1989	Gilroy Array #3	CDMG	0.56	0.892
Superstition Hills	1987	Poe Road (temp)	USGS	0.45	1.126
Cape Mendocino	1992	Rio Dell	CDMG	0.55	0.909

Table 3. Specifications of bearing used.

Surface 1	$d_1 = 91\text{mm}$	$R_{\text{eff}1} = 870\text{mm}$	Series element 1	$\bar{d}_1 = 80\text{mm}$	$\bar{R}_{\text{eff}1} = 212\text{mm}$
Surface 2	$d_2 = 27\text{mm}$	$R_{\text{eff}2} = 106\text{mm}$	Series element 2	$\bar{d}_2 = 80\text{mm}$	$\bar{R}_{\text{eff}2} = 764\text{mm}$
Surface 3	$d_3 = 27\text{mm}$	$R_{\text{eff}3} = 106\text{mm}$	Series element 3	$\bar{d}_3 = 80\text{mm}$	$\bar{R}_{\text{eff}3} = 764\text{mm}$
Surface 4	$d_4 = 91\text{mm}$	$R_{\text{eff}4} = 870\text{mm}$			

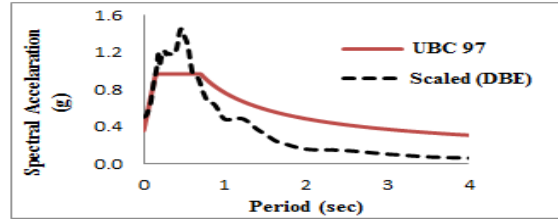


Figure 7. Average 5% damped spectral acceleration of SS ground motions and design spectra.

5. COMPARISON OF RESULTS

Results are shown in story shear, story drift, structural displacements and hysteresis curves of isolators. Each curve is averaged of nonlinear time-history response of seven records. Results of this research have been compared with similar research (Ryan & Earl, 2010)

The modal inertial force distributions were obtained by modal analysis, and are plotted for each mode normalized by the mass at each level (Fig. 8). As a result of the period shift, the spectral acceleration or base shear is reduced, while the increased deformations are accommodated by the isolation system. Deformation of the isolation system simulates the shape of the first or fundamental mode, while the higher modes containing structural deformation have very limited participation. As it could be suggested, reference structure (curve. g in fig.8) has the maximum acceleration in first mode, and more over other primary modes have significant acceleration.

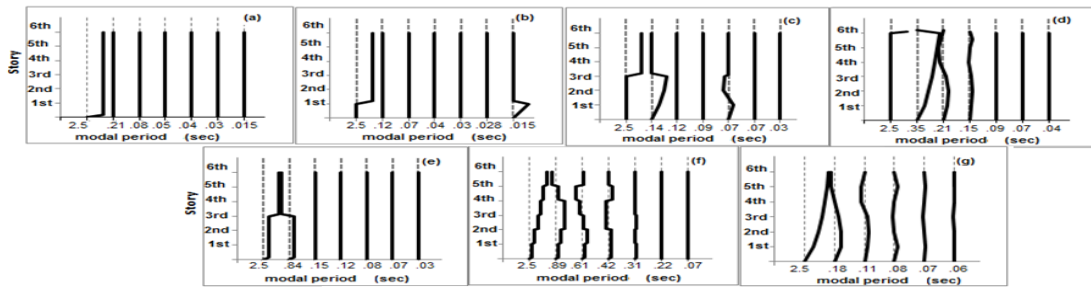


Figure 8. Modal expansion of inertial forces for frames with inter-story isolation at: (a) the base; (b) the first story; (c) third story; (d) the roof; (e) base and third story; (f) every story; and (g) fixed-base

Base-isolation system (curve a), has significant effect for decreasing of applied acceleration. Because applied acceleration is restricted to first mode so drifts for other modes are negligible and applied load on connections will be less. In case of isolator in first story (curve b) acceleration is decreased and bounded to first mode and only a little of moment participation can be seen in higher modes. When isolator is located in third story (curve c), applied acceleration on upper part (above isolators) will be minimum and total moment will be absorb by this part and lower part do not participate in first mode. In this case lower part of isolation level which supported on ground, absorbs significant amount of acceleration in second mode. The pattern of modal inertial forces in the roof isolated frame is similar to the fixed-base frame,

with contributions in several of the higher modes. In case of isolator in all stories (curve f) the pattern is same as reference structure (curve g), because isolated stories behave flexible and structure elements like semi-rigid connections have negligible displacements.

The displaced shapes for both DBE and MCE earthquakes that result by combining median peak isolator deformations and inter-story drifts are shown for the various isolated frames in Fig. 9(i) and 10(ii). Each curve has been derived from average of seven curves for DBE and MCE levels. Displaced shapes in MCE level are 1.5 times greater than DBE level.

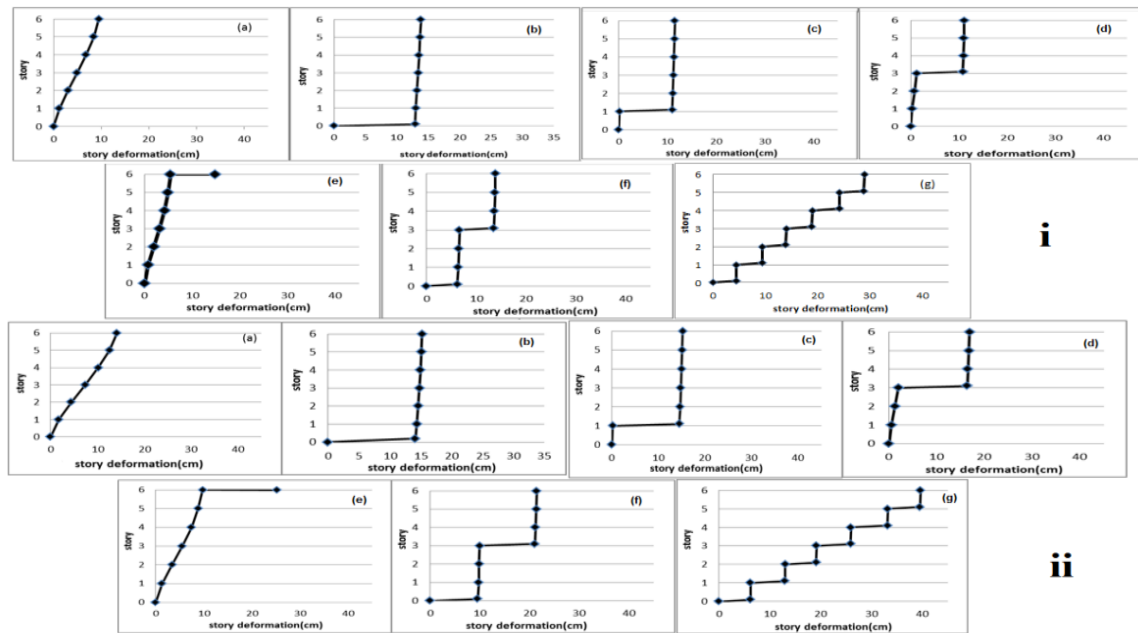


Figure 9. Structural displaced shapes for (i) DBE level (ii) MCE level, (a)reference structure with fixed base; Isolated structure at (b) base;(c) first story;(d) third story;(e) roof;(f) base and third story; and (g) every story.

Isolator in each story decreases drift for upper part significantly, but lower part's drifts have not been affected. This matter can be seen when isolator located in third story (curve d), in this case lower part's drifts have been decreased % 40-%50 in comparison with reference structure. When isolators installed in several stories (curve f and g) drifts will be decreased for all stories; deformation demands decrease in multi-story isolation systems, since the essentially constant spectral deformation demand is shared by isolators at multiple stories. This effect can be used in near-fault areas, which drift demand caused by earthquake is high, this matter is clear in curve g which has maximum drifts between seven cases.

Comparison between story shears of this research and the similar research on rubber bearings (LRB) (Ryan & Earl, 2010) are shown in figure10. Story shears for both DBE and MCE are approximately the same, because horizontal axis of charts has been normalized with base shear of reference structure and we used only DBE curves. As is clear, two charts are matched properly. Story shear in sixth story is about 30% of base shear for fixed-base structure (reference structure) and for lower stories, this value increases, finally it will be equal to base shear in first story as expected. As an important conclusion, isolation at first story decreases story shear as much as base isolation system. Story shears in the third story and roof-isolated frames are greater than in the base-isolated frame, but still reduced compared to the fixed-base frame. In the base isolation, first story isolation and both systems have multi-level of isolation; value of base shear has a significant reduction (about %80-%85 of corresponding values in the reference structure with fixed base). Relative to base isolation, isolation at third story leads to comparable reduction in superstructure response above the isolation level but an increase below the isolation level. Isolation at

roof, which is essentially a tuned-mass damper (TMD), has the least effect for decreasing in story shear (only 20% - 25% decrease in story shear).

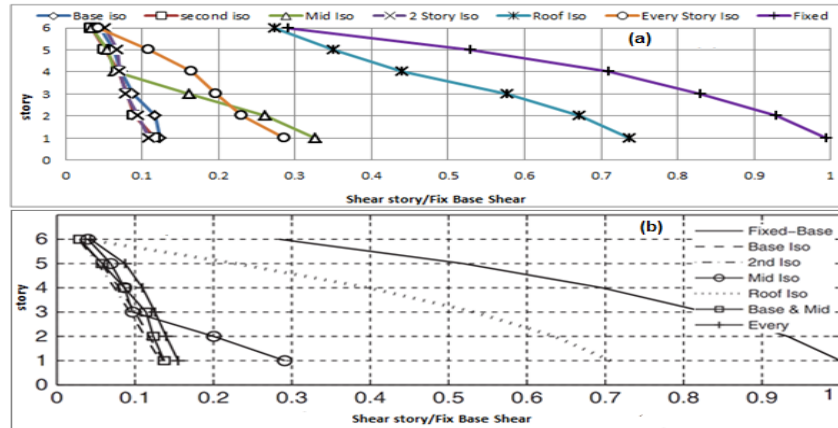


Figure 10. Story shear normalized by base shear in (a) this research (b) similar research on LRB (Earl, 2007).

Inter-story drifts are illustrated in figure 11. As it can be derived, inter-story drifts in MCE level are 1.5 times greater than those for DBE level. In reference structure (fixed-base), inter-story drifts starts from a certain value in first story, ascend till third story, then descend in next three stories and it will be less than the value in first story. This case is repeated for roof-isolation system. In conclusion, isolation at first story decreases inter-story drifts as much as are even more than base isolation system, especially drifts in first story which has been decreased about 50%. Simultaneously isolation at base and third story levels doesn't have a significant effect on decreasing in inter-story drifts in comparison with base isolation system. Installing one more isolation level at third story has only a minor effect on drift decreasing in upper part. Isolation at third story decreases inter-story drifts significantly, although the first three stories are connected to ground. Isolating structure at roof, decreases inter-story drifts for lower parts 30% in comparison with reference structure in DBE earthquake, and there is the same rule for MCE level. Generally roof isolation system or tuned mass damper (TMD) doesn't have a good performance for decreasing of inter-story drift and story shear in comparison with other isolation systems.

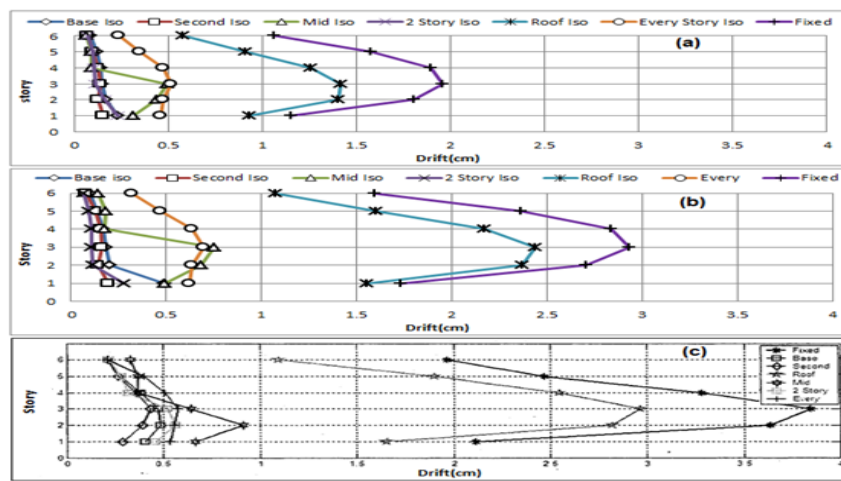


Figure 11. Inter-story drift for (a) DBE level; (b) MCE level; (c) similar research on LRB (Ryan & Earl, 2010).

It is important to note that the distribution of story drifts Δ_i differ from that of story shears since the story stiffness k_i was reduced every two stories and $V_i = k_i \cdot \Delta_i$.

Hysteresis curves of isolators for DBE level are shown in figure 12 and for MCE in figure 13.

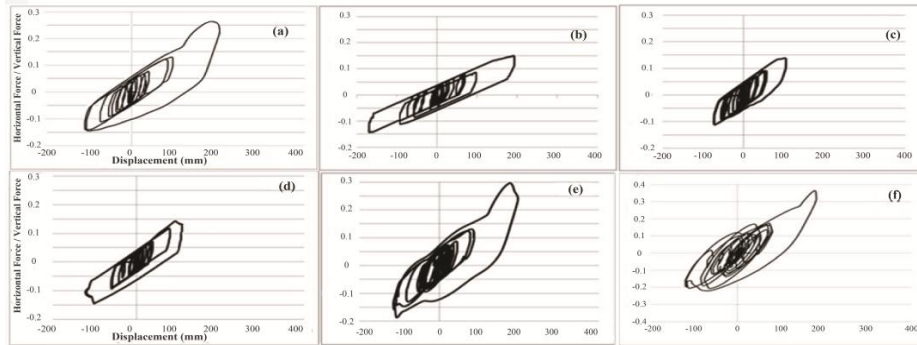


Figure 12. Hysteresis curves of isolators at DBE level for isolated structure at (a) base; (b) first story; (c) and (d) simultaneously isolation at base and third story; (e) third story; and (f) roof.

Damped energy for roof isolation is more than other isolation systems this would confirm the performance of TMD systems. Crossing point between curves and vertical axes is friction coefficient, friction coefficient are 0.06-0.13 (the same values were initially considered). If isolators are installed at base, their hysteresis curves contain broken regular lines and are like parallelogram, when isolators are installed at upper levels, regularity of curves decreases and isolators will not work with their maximum capacities. At DBE level as is clear in curves, isolators will work only until their third sliding regime and isolators will not use all their capacities. When isolators are working at MCE level, and they are installed at base or first story, all five sliding regimes would work (see fig. 2) and isolator performance will be optimum. When the outer slide plates contacts the displacement restrainers, inclined lines appear in hysteresis curves which represent the fifth sliding regime has started. As long as the isolator is installed at a higher level, optimum performance will be reduced and sliding regimes of isolators will not be complete. For example in third-story isolation system (curve (e) in fig.13), only a few percentage of fifth sliding regime is engaged. When isolators are installed at base and third story simultaneously, sliding regimes of isolators will not be complete since the essentially constant spectral deformation demand is shared by isolators at multiple stories.

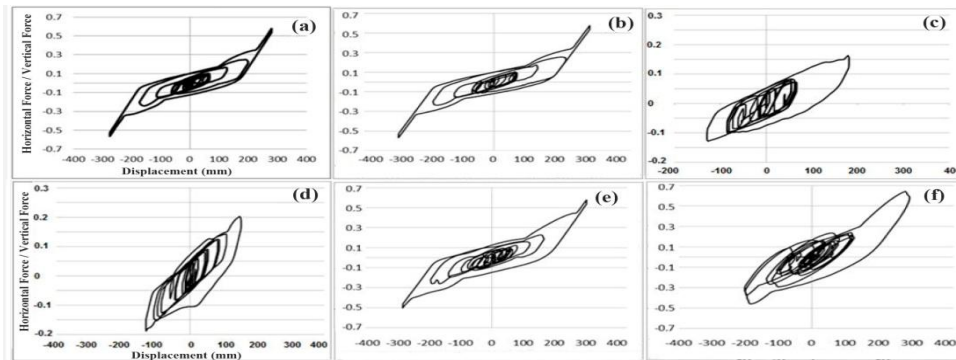


Figure 13. Hysteresis curves of isolators at MCE level for isolated structure at (a) base; (b) first story; (c) and (d) simultaneously isolation at base and third story; (e) third story; and (f) roof.

6. CONCLUSION

This research has evaluated the effectiveness of installing Triple Friction Pendulum Bearing (TFPB) in the different levels of the structure. And also seismic response of each case is compared with fixed-based frame and base isolated frame. The specifications of the bearings were selected such that all isolated frames had the same fundamental period of 2.5sec at the design deformation. The results of the research are summarized as below:

Moving the isolation level from base to first story has an extraordinary effect on mitigating the story acceleration (inertial force), story shears and story drifts, and in some cases it works even better than base isolation system. Such practice could be beneficial for a variety of applications such as buildings with irregular first stories (parking structures), changing in column arrangement, work abilities and architectural design of upper part and lower part of isolated level. Widespread application of isolation in high story of structures depends on the development of alternative aesthetically appealing and economical methods for accommodating the isolation plane and the seismic gap within the building architectural.

Implementation an isolated system in a level is effective in reduction of the force demands above the isolation system but has less effect on reduction of the force demands in lower levels. With increasing installation level, the overall effect of this system will be reduced. Although roof isolation has the least effect in inter-story isolation systems, but has relatively large effect on decreasing seismic response of a fixed-base structure. Installing roof isolation system could be an economical option for retrofitting an existing building. But softer isolation systems have better operation than triple pendulum since such these bearing are designed for high axial force. A multi-story isolation system such as two isolated stories or isolation at every story is extremely effective but obviously it is not economical. This system can be used just for very important structures with the most likely existence of near-fault ground motion. Since the essentially constant spectral deformation demand is shared by isolators at multiple stories.

Accurate selecting dynamic specifications of triple friction pendulum bearing, has a significant effect on its performance, so that if these features are determined through accurate calculations, while the adaptive behavior of bearing doesn't disrupt, Proportional to the applied earthquake DBE or MCE, bearing has shown the optimal behavior. As long as the bearing is installed at a higher level, sliding regimes of isolators will not be complete and only a few percentage of sliding regimes are engaged.

REFERENCES

- Fenz, D., Constantinou, M. (2008). Modeling Triple Friction Pendulum Bearings for Response-History Analysis. *Earthquake Spectra*. **24:4**,1011-1028.
- Ryan, K., Earl, C. (2010). Analysis and Design of Inter-Story Isolation Systems with Nonlinear Devices. *Journal of Earthquake Engineering*. **14**, 1044-1062.
- Constantinou, M., Fenz, D. (2008). Mechanical Behavior of Multi-spherical Sliding Bearings. MCEER-08-0007.
- Charnpis, D., Komodromos, P. (2012). Optimized earthquake response of multi-storey buildings with seismic isolation at various elevations. *EARTHQUAKE ENGINEERING & STRUCTURAL DYNAMIC*. DOI: **10.1002/eqe.2187**.
- Shirayama, A., Yamashita, T., Ito, S., Mukai, Y., Baba K., and Inoue, Y. (2004). Design proposal for controlling seismic behaviors of inter-story isolation building structures 13th World Conference on Earthquake Engineering, Vancouver, B.C., Canada, August 1-6, 2004